Satellite-Derived Equilibrium Lines in Northern Patagonia Icefield, Chile, and Their Implications to Glacier Variations

Authors: Barcaza, Gonzalo, Aniya, Masamu, Matsumoto, Takane, and Aoki, Tatsuto

Source: Arctic, Antarctic, and Alpine Research, 41(2) : 174-182

Published By: Institute of Arctic and Alpine Research (INSTAAR), University of Colorado

URL: https://doi.org/10.1657/1938-4246-41.2.174

Arctic, Antarctic, and Alpine Research, Vol. 41, No. 2, 2009, pp. 174–182

Satellite-Derived Equilibrium Lines in Northern Patagonia Icefield, Chile, and Their Implications to Glacier Variations

*Gonzalo Barcaza**§
*Masamu Aniya**
Takane Matsumoto† *and*
Tatsuto Aoki‡

*Graduate School of Life and Environmental Sciences, University of Tsukuba, Ibaraki 305-8572, Japan
†Research Center for Natural Hazards and Disaster Recovery, Niigata University, Niigata 950-2181, Japan
‡Department of Geography, Kanazawa University, Kanazawa 920-1192, Japan
§Corresponding author: gbarcaza@uc.cl

Abstract

The Northern Patagonia Icefield (NPI), covering 3953 km^2, is the second largest temperate ice body in South America. Despite its importance as a climate change indicator because of its location and size, data on ground-based mass balance and meteorological records for the analysis of glacier (snout) variations are still lacking. The use of multitemporal satellite images to estimate equilibrium line altitude variations could be a surrogate for such analyses. Since late-summer snowlines of temperate glaciers coincide with the equilibrium line, we analyzed five Landsat images spanning 1979–2003 and an ASTER-derived digital elevation model to reveal oscillations in the equilibrium line altitude (ΔZ_{ELA}). The average ELAs range between 870 m and 1529 ($\pm$ 29 m), with lower altitudes on the west side. Winter snow cover accumulation indicates higher elevations (relative to the glacier snout) of the transient snowlines in the west. Thus, one of the reasons for the higher retreating rates observed on the west side is that the lower part of the ablation area is likely exposed to year-round ablation. Glacier sensitivity to ΔZ_{ELA} oscillations would depend upon the topographic condition of the accumulation area (gentle or steep). In outlet glaciers with gentle accumulation areas such as San Rafael and San Quintin, ΔZ_{ELA} of up to 65 and 70 m at the central flow part and bare ice area variations $>$ 5 km^2 and $>$ 13 ($\pm$ 0.6 km^2) were observed, respectively.

DOI: 10.1657/1938-4246-41.2.174

Introduction

In Patagonia there are two large temperate ice bodies that together cover about 16,950 km^2. They are the Northern Patagonia Icefield (NPI), with 3953 km^2 (Rivera et al., 2007); and the Southern Patagonia Icefield (SPI), with 13,000 km^2 (Aniya et al., 1992). Despite their importance as climate change indicators and their contribution to sea-level rise (Aniya, 1999; Rignot et al., 2003; Rivera et al., 2007) in the southern hemisphere, current knowledge of their glacier variations and response to global warming is still very limited.

Glacier variations of the NPI's 21 major outlet glaciers were elucidated by Aniya (2007), who observed a general retreat over the 60 years from 1944/1945 (austral summer) to 2004/2005. Glacier retreat in Patagonia has been interpreted as a response to global warming and, to a lesser extent, to a decrease in precipitation (Aniya, 2001; Casassa et al., 2002; Aniya, 2007).

Ground-based year-round mass balance records and long-term meteorological data at or even near glaciers are scanty in Patagonia (i.e., Yamada, 1987; Matsuoka and Naruse, 1999; Shiraiwa et al., 2002; Rivera et al., 2005). Although remote sensing techniques could be an effective means of correlating glacier variations with changes in glacier surface conditions (shift of the equilibrium line [EL]; bare ice or snow cover), in Patagonia the unknown glacier surface conditions (or the lack of ground-truth data) at the time of image acquisition may be a drawback (De Angelis et al., 2007). However, this is a common problem in the EL definition (i.e., Williams et al., 1991; Klein and Isacks, 1999; Khalsa et al., 2004).

Since different glacier facies can be detected on Landsat images (Williams et al., 1991), both the maximum ablation and the maximum snow cover accumulation can be analyzed through satellite monitoring. Since late-summer snowlines of temperate glaciers can be taken as the EL, we can also derive the equilibrium line altitude (ELA) by combining this data with a digital elevation model (DEM).

The ELA, the boundary that separates the accumulation area from the ablation area (Paterson, 1994), was employed in this study because it links glacier response and climate change (Kuhn, 1989; Ohmura et al., 1992). When using winter images, the transient snowline (TSL) indicates the outer limit of retained winter snow cover accumulation.

The ELAs of the entire NPI were previously estimated by Aniya (1988) using aerial photographs taken in March 1975 and topographic maps from the same year. In the SPI, a mid-summer mosaic (14 January 1986) of the Landsat Thematic Mapper (TM) was used to locate the EL (Aniya et al., 1996).

Taking the NPI as the study area and using Landsat images, the objectives of this study are: (1) to estimate the ELAs and interannual bare ice area variations; (2) to derive winter transient snowlines; and (3) to analyze satellite-derived ELAs and TSLs to discuss the glacier variations in the NPI. We used five late-summer and two winter Landsat Multispectral Scanner (MSS), Thematic Mapper (TM), and Enhanced Thematic Mapper (ETM+) images, together with aerial surveys from 2004, 2005, and 2007. Ground meteorological data, although scanty, were used for analyzing the altitude of the 0°C isotherm.

Study Area

The NPI stretches between 46°30′S and 47°30′S along 73°30′W, and is the source of some 28 major outlet glaciers

1523-0430/09 $7.00

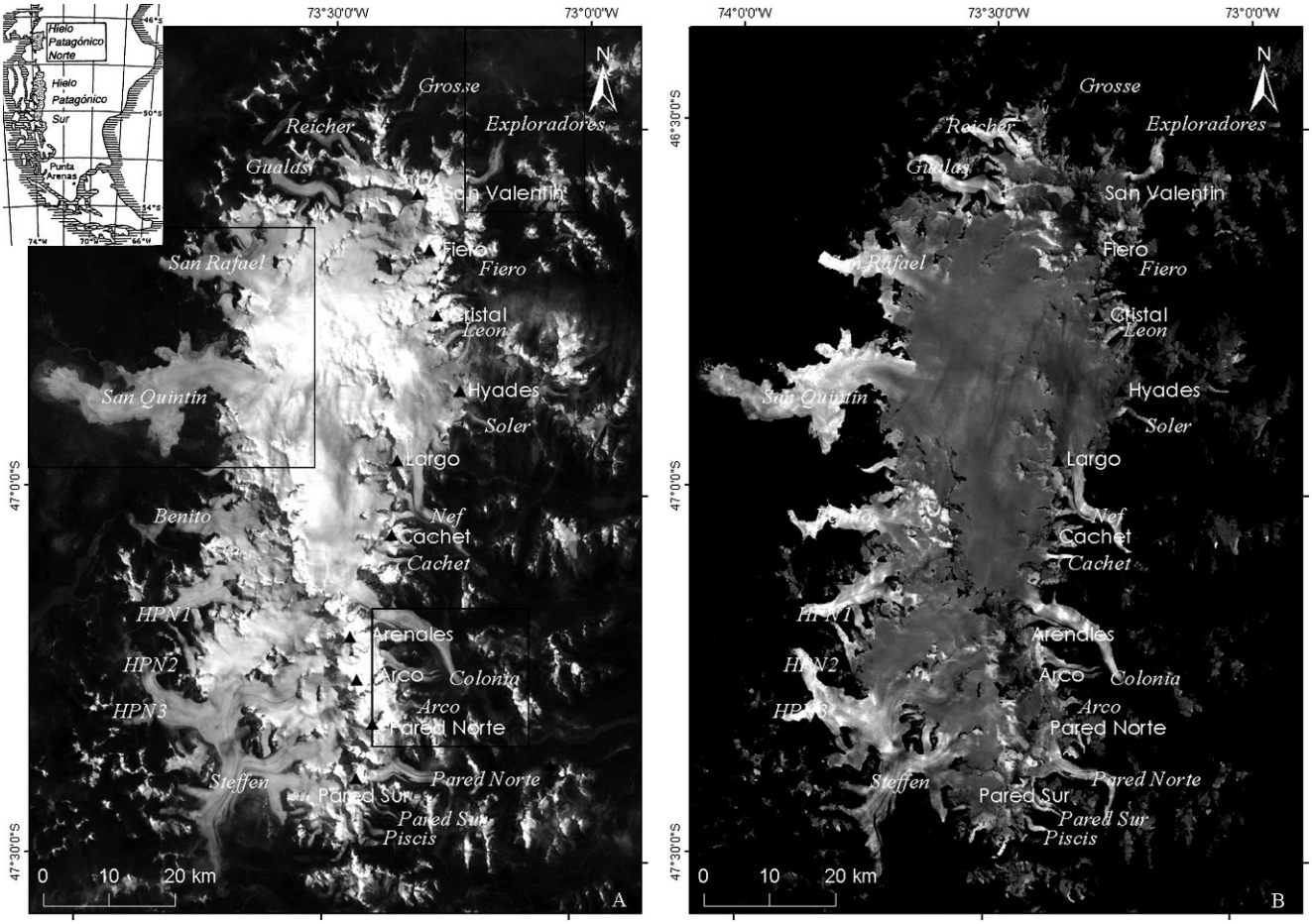

FIGURE 1. (A) Landsat ETM+ (02 April 2003) of the Northern Patagonia Icefield showing its outlet glaciers. Inset indicates the location of the Patagonia icefield and the study area. Location of Exploradores, San Rafael, San Quintin, and Colonia glaciers is indicated by box. (B) Using a normalized difference index (NDI) with red (TM3: 0.58–0.68 μm) and near infrared (NIR) (TM4: 0.75–1.1 μm) bands, the accumulation (darker) and ablation (lighter) areas are separated. Glacier names indicated in italic, while mountain names in gothic type.

(Aniya, 1988) (Fig. 1A). It extends for about 100 km from the Grosse to the Steffen glacier and has a width of over 40 km between the San Quintin (west) and Colonia (east) glaciers.

On the east side, several peaks emerge from the icefield south of San Valentin (3910 m), which is the highest mountain in Patagonia (Fig. 1A). Outlet glaciers located on the west side of the NPI are in general both gentler and longer than those located on the east side.

As a result, a marked east–west climatic gradient between the maritime climate on the west side and the drier climate on the east side of the NPI has been widely recognized (Ohata et al., 1985; Inoue, 1987; Warren and Sugden, 1993; Kerr and Sugden, 1994). Mass balances derived from ice cores recovered from the NPI (Yamada, 1987; Matsuoka and Naruse, 1999) also support this east–west climatic gradient.

Most of the outlet glaciers of the NPI have been retreating and thinning at high rates since 1944/1945 (Aniya, 1999; Rignot et al., 2003; Aniya, 2007; Rivera et al., 2007). Glacier variation studies have revealed a wide variety of variation factors in Patagonia, including calving (Warren and Sugden, 1993; Naruse et al., 1995; Warren et al., 1995; Warren and Aniya, 1999; Aniya, 2007), debris cover (Aniya, 1992; Wada and Aniya, 1995), and fjord topography (Aniya, 2007).

Data and Methods

We used five late-summer Landsat images to derive the EL and interannual bare ice area variations (Table 1). They span from 1979 to 2003 with irregular time spacing due to the availability of suitable images. In addition, two winter ETM+ scenes (1999 and 2004) were used to derive the winter bare ice area. In this paper, interannual bare ice area variations are defined by changes in the glacier surface conditions due to oscillation of the ELA, and the high variability of the snowline is estimated by the range of its variation (ΔZ_{ELA}).

Based upon late-summer images, satellite-derived snowlines may be assumed to coincide with the EL, because in temperate glaciers such as those of Patagonia (Yamada, 1987; Shiraiwa et al., 2002) the formation of superimposed ice is insignificant (Paterson, 1994). In order to estimate the ELA, the average altitude of the EL was computed using the DEM. By comparing the two consecutive data, upward ΔZ_{ELA} means an increase in the bare ice area, while downward ΔZ_{ELA} means a decrease in the bare ice area.

IMAGE PRE-PROCESSING

Radiometric calibrations, orthorectification, DEM generation, and all image manipulations were carried out using the Research Systems Inc. (RSI) Environment for Visualizing Images (ENVI) computer software. We used the sensor metadata to convert digital numbers to radiance (W m^{-2} $ster^{-1}$ μm^{-1}) using gain and offset, and then to top-of-atmosphere (TOA) reflectance (ρ_p, unitless planetary reflectance).

TABLE 1

Landsat imagery used to estimate the equilibrium lines altitudes of the Northern Patagonia Icefield.

Sensor	Path/Row	Date	Season	Sun Elevation	Sun Azimuth
MSS	248/093	08 March 1979	Late summer	30.13	61.5
TM	232/092–093	07 March 1985*	Late summer	32.54	58.2
ETM+	232/092–093	08 March 2000	Late summer	34.9**	52**
ETM+	232/092–093	11 March 2001	Late summer	33.9**	51.8**
ETM+	232/092–093	02 April 2003*	Early autumn	27.6	45.7
ETM+	232/092–093	12 July 1999	Winter	12.3**	36.8**
ETM+	232/092–093	25 July 2004	Winter	14.1**	39**

* Images acquired in mosaic mode from the U.S. Geological Survey.

** Value for row 093.

In the absence of ground-truth information during image acquisition, an image-based dark object subtraction (DOS) technique (Chavez, 1988) was employed to convert TOA reflectance to surface reflectance (hereafter reflectance). Then, pixel brightness variations due to solar elevation were corrected based upon the cosine law (Rees, 2006, p. 154).

All the Landsat images were orthorectified using rational polynomial coefficients (RPC) and about 25 ground control points (GCPs) together with a DEM (see DEM section), resulting in a root mean square error (RMSE) of about one pixel. We resampled all the images to a 30-m pixel size using the nearest neighbor algorithm, with the UTM projection and the South American Datum.

To avoid the misidentification of water bodies packed with icebergs as glacier ice, a snow and ice mask was created, and thin clouds over the icefield were clipped out by using the normalized difference snow index (NDSI) with a threshold value of 0.4 (Dozier, 1989).

DERIVATION OF THE EQUILIBRIUM LINE (EL) AND IMAGE NORMALIZATION

To discriminate bare ice from snow, we used a normalized difference index (NDI) with red and near infrared (NIR) bands (e.g., Boresjö and Bronge, 1999). The algorithm enhances reflectance differences between bare ice and snow, resulting in an NDI image in which the accumulation area (snow facies) stands out as dark due to the lower values, whereas the ablation area (ice facies) stands out as bright due to the higher values (Fig. 1B). Bright spots in the accumulation area due to a shadow effect were not a problem for delineation of the ablation area.

The correction of the influence of non-surface factors such as the sun angle, atmospheric conditions, and sensor geometry (Heo and FitzHugh, 2000), which is required for multitemporal analyses, was carried out with a radiometric normalization by adjusting all the NDI images to the ETM+ 2003 NDI (Table 2). This procedure ensures consistency of the bare ice definition.

TABLE 2

Regressions for image normalization obtained for the normalized difference index image data based on ETM+2003.

Image	Linear regression	R^2
MSS 1979	$y = 0.6579x + 0.0142$	0.9498
TM 1985	$y = 1.1136x - 0.024$	0.914
ETM+ 2000	$y = 0.6748x + 0.1308$	0.9492
ETM+ 2001	$y = 1.2108x + 0.0806$	0.9612
ETM+ 1999	$y = 1.0535x + 0.1313$	0.9014
ETM+ 2004	$y = 1.2568x + 0.1276$	0.9398

DIGITAL ELEVATION MODEL

We created a DEM of the NPI using an Advanced Spaceborne Thermal Emission and Reflection Radiometer (ASTER) mosaic from 2002 data (Table 3). DEM creation followed the standard procedure, which included epipolar image creation, image-matching, parallax-matching, and parallax-to-DEM conversion. In addition, it was post-processed to remove artifacts and smoothed with low-pass convolution (5×5 kernel). Based upon topographic maps from 1975, the vertical accuracy of the ASTER DEM ($RMSE_Z$) is ± 29.3 m.

DERIVATION OF THE EQUILIBRIUM LINE ALTITUDE (ELA)

Based upon the NDI-normalized images, we performed a *k*-means unsupervised classification, the result of which was grouped into five classes: non-ice; shadow; bare ice; slush; and wet snow. We delineated the ablation area by aggregating pixels classified as bare ice, and the ELA was estimated with the DEM. Using an unsupervised classification (Aniya et al., 1996) in the 2001 image, the estimated error is about $0.6 \pm$ km^2. In order to derive interannual bare ice area variations, we counted the difference between pixels classified as bare ice within a matching region of interest around the EL. However, when the EL meanders across the glacier surface over a diverse range of elevations, the assignment of an altitudinal value is a problem for estimating the ELA (Chinn et al., 2005). Altitudinal oscillation of the ELA (ΔZ_{ELA}) is the difference between two observation periods.

AERIAL SURVEYS

Winter aerial surveys carried out on 25 July 2004 and 15 August 2005 revealed that the outlet glaciers located on the north, west, and south sides of the NPI (see Fig. 1A) were free of snow at the lower part of the ablation area. On the other hand, those located on the east side of the icefield were found to be almost

TABLE 3

ASTER data for digital elevation model generation of the Northern Patagonia Icefield.

Acquisition date	Area covered
10 February 2002	Main Plateau (north)
10 February 2002	Main plateau (south)
02 May 2000	San Quintin glacier (snout)
17 February 2002	Grosse and Exploradores glaciers
03 September 2001	San Rafael and San Quintin (ablation area)

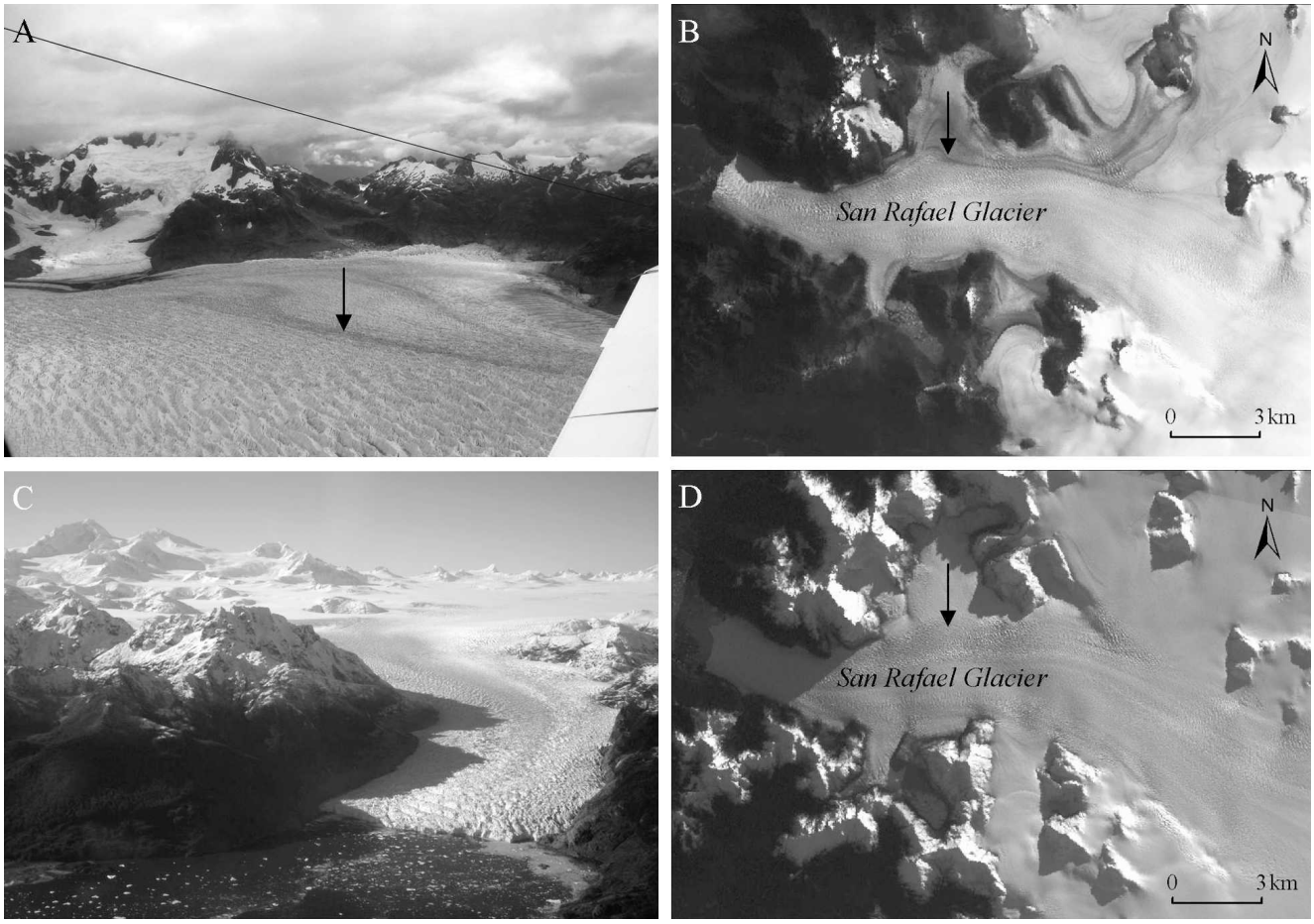

FIGURE 2. Surface conditions for San Rafael Glacier (ca. 760 km^2) between late summer ([A] 05 March 2007; [B] ETM+, 02 April 2003) and winter ([C] 15 August 2005; [D] ETM+, 12 July 1999). Near-maximum melting conditions on glacier surface are indicated by moraines (marked with arrows) that have emerged in late-summer due to snow-cover melting. In the far back of C is Monte San Valentin (3910 m), the highest mountain of Patagonia (photo by M. Aniya on 25 July 2004).

completely covered by snow all the way down to the lowest altitudes of their ablation area.

The late-summer aerial survey carried out on 05 March 2007 showed ELA similar to those of the satellite-derived ELAs, and debris cover, nunataks, and moraines in the ablation areas were at maximum exposure (Figs. 2 and 3).

METEOROLOGICAL DATA

Field measurements of air temperature and precipitation in front of Exploradores Glacier (elevation 196 m) started in December 2003 (Aniya et al., 2007). Mean monthly temperatures of 9.4°C in March and 3.9°C in July were recorded during 2005, with persistent precipitation throughout the year (3260 mm in 11 months). Freezing temperatures were reached sporadically during fall (May) but more systematically in winter. A daily mean temperature of −1.1°C was registered at the time of ETM+ image acquisition on 25 July 2004.

The altitude of the 0°C isotherm was estimated based upon the meteorological data at the Exploradores Glacier using a lapse rate of 0.53°C/100 m (Inoue et al., 1987). It was located around 2000 m and 900 m for late-summer and winter conditions, respectively. The summer value agrees with freezing levels derived from radiosonde observations at San Rafael Glacier (Fujiyoshi et al., 1987).

Results and Discussion

EQUILIBRIUM LINE ALTITUDE

A summary of the satellite-derived ELAs, together with those estimated by Aniya (1988), is presented in Table 4. For some glaciers with a complex accumulation area such as Colonia and Nef, only the outlet coming from the plateau (icefield) is presented. HPN 2 and HPN3 glaciers are not included because the boundaries of their accumulation areas are not well defined (Aniya, 1988). On the east side of the NPI, at León Glacier, pixels classified as bare ice were found in a crevassed zone with a diverse range of elevations, because this glacier is nourished from the icefield through ice falls; at Fiero Glacier, classification was possible only for 2003.

The average ELAs range between 870 m and 1529 (± 29 m) while ΔZ_{ELA} oscillations range between 11 m and 376 (± 29 m) over the 24 years from 1979 to 2003. The large difference in ΔZ_{ELA} is a clear indicator of the high spatial and temporal variability of snow accumulation (see Table 4). In general, lower ELA elevations and larger bare ice area variations were found in outlet glaciers located on the west and south sides of the NPI, which may be attributed to a large accumulation area (length of the glacier) and the orographic effect (Ohata et al., 1985). Figure 4 depicts the Landsat classification results for the two largest glaciers, San Rafael and San Quintin. On the east side of the NPI, higher ELA

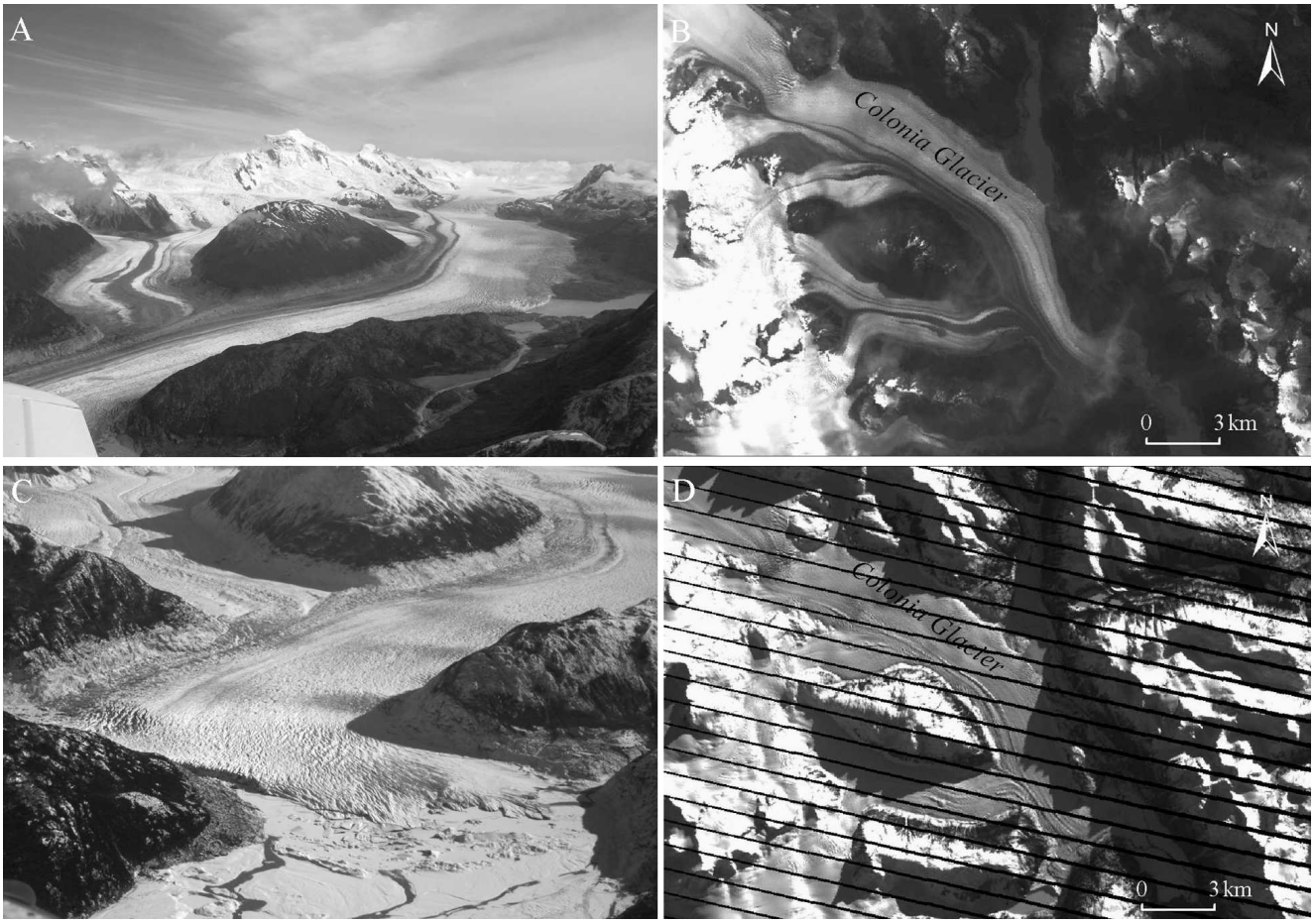

FIGURE 3. At Colonia Glacier (ca. 437 km^2), late-summer conditions ([A] 05 March 2007; [B] ETM+, 02 April 2003, TM1) yielded an averaged ELA of 1270 m. On 25 July 2004, the transient snowline came down to an elevation of 140 m covering completely the ablation area ([C] photo by M. Aniya; [D] ETM+, TM1). Proglacial lake is seen to be frozen. In the far back of photo A is Cerro Arenales (3365 m). Note: Scan Line Corrector anomaly of ETM+ 2004.

elevations and smaller bare ice area variations were found. This east–west contrast in the observed ELA (1979–2003) agrees with the rise in altitude of the ELA; as the position of the EL moves away from the Pacific Ocean, precipitation decreases (Kerr and Sugden, 1994).

Error factors in the satellite-derived ELAs include the acquisition time and pixel size of images and the grid size of a DEM (Rabatel et al., 2005). The uncertainty in the ELAs for 1979 and 1985 may be related to the prolonged thinning of the NPI, which is estimated at 1.0 ± 0.10 (m yr^{-1}) between 1975 and 2000 (Rignot et al., 2003). However, although elevation changes have higher spatial variability (Rivera et al., 2007), surface changes in bare ice greater than 10 km^2 on the west and south sides and 1 km^2 on the east side of the NPI are interpreted as shifts in the ELA due to ice thinning (Fig. 5).

The uneven impact of ΔZ_{ELAs} on the bare ice variations results from both the size of the glacier and the location of the ELA, i.e., over gentle or steep accumulation areas. The glacier surface slope around the ELA is indicated in Table 4. At San Rafael Glacier, interannual bare ice area variations of up to 5.22 ± 0.6 km^2 were observed. Large variations, i.e., greater than 10 km^2, were found on the west and south sides at larger outlet glaciers with a gentle accumulation area, such as San Quintin and Steffen glaciers. On the east side, larger outlets such as Colonia and Nef glaciers varied more than 3 km^2, while smaller ones such as Piscis, Arco, Cachet, and Soler glaciers varied less than 1 km^2. Therefore, slight ΔZ_{ELA} has an uneven impact on the variation of the bare ice area in larger outlet glaciers if the ELA meanders across the width of the glacier over wide and gentle accumulation areas.

WINTER TRANSIENT SNOWLINE

During winter seasons, the extent of satellite-derived bare ice in 1999 and 2004 as well as the aerial surveys on 25 July 2004 and 15 August 2005 indicate that the larger bare ice areas in winter were found on the outlet glaciers located on the north, west, and south sides, whereas smaller bare ice areas in winter were found on the east side of the NPI (Table 5).

At San Rafael Glacier, bare ice areas exposed in the winters of 1999 and 2004 were about 14.9 km^2 and 11.4 (± 0.6 km^2), comprising 8.5% and 6.5% of its ablation area, respectively. Although a daily mean temperature of −1.1°C was recorded at Exploradores Glacier on 25 July 2004, the lower part of the ablation area of San Rafael Glacier was observed to be snow free and its TSL was found at an elevation of 440 m even when the 0°C isotherm was located near sea level. On the other hand, at Colonia Glacier snow cover remained over the entire ablation area, suggesting faster snow cover melting on the west side as a result of warmer conditions (see Figs. 2 and 3).

At San Quintin Glacier in 1999, the TSL was located at 510 m with a bare ice surface of 151 ± 0.6 km^2, which is 37.5% of its

TABLE 4

Satellite-derived equilibrium lines altitudes (m) between 1979 and 2003 in Northern Patagonia Icefield.

Glacier Name	*1975**	1979	1985	2000	2001	2003	Average 1979–2003	ΔZ_{ELA}	Slope**
Northern Side									
Grosse	*950*	nd	nd	1211	1145	1316	1224	171	29
Western Side									
Reicher	*850–950*	nd	nd	1524	1535	1530	1529	11	12.5
Gualas	*750–900*	970	1060	985	970	999	996	90	16
San Rafael	*1200*	905	903	897	903	895	900	10	1.6
San Quintin	*1200*	950	960	950	960	929	950	31	1.2
Benito	*1150*	870	900	856	815	940	876	125	1.1
HPN 1	*1100*	1000	1054	917	678	840	897	376	1.7
Southern Side									
Steffen	*900–1000*	980	1054	978	1000	998	1000	76	1.6
Eastern Side									
Piscis	*1000*	1190	1130	1133	1139	1116	1141	74	13
Pared Sur	*800–850*	920	913	822	826	nd	870	98	31
Pared Norte	*900–1000*	996	1061	***	1000	1023	1020	65	4
Arco	*1250*	1398	nd	1330	1264	1346	1335	134	8.8
Colonia	*1300–1250*	1222	1282	1282	1328	1245	1270	106	1.3
Cachet	*1350–1100–1200*	1309	1356	1354	1347	1350	1343	47	8.9
Nef	*1350*	1218	1337	1245	1251	1197	1250	140	4.4
Soler	*1350*	1350	1398	1407	1423	1374	1390	73	13.1
León	*1350*	1280	1580	1579	1544	1407	1478	300	7.8
Fiero	*1100–1000*	nd	nd	***	***	1110	—	—	—
Exploradores	*1250*	nd	nd	1555	nd	1470	1512	85	13.1

*From Aniya (1988) ** degrees *** no result.
nd: no data.

ablation area; however, in 2004 it had descended to an elevation of 257 m, suggesting a large snow cover variation due to the glacier length and its gentle ablation area (Fig. 6). Winter bare ice areas of San Rafael and San Quintin glaciers suggest that the difference in the snow-free area in winter in the ablation area may have been responsible for the recent snout disintegrations of San Quintin Glacier, in which the breaking-away is mainly due to accelerated melting/calving of its near-floating snout (Aniya, 2001).

IMPLICATIONS FOR GLACIER VARIATIONS

In the NPI, Aniya (2007) reported a general retreating trend between 1944/1945 and 2004/2005 with some episodes of small advances (i.e., San Rafael Glacier). The total front area lost at 21 major outlet glaciers in 60 years is about 101.36 km^2, of which the two largest outlet glaciers account for 41.44 km^2: San Quintin glacier with 28.8 km^2 and San Rafael with 12.64 km^2. However, the large retreat undergone by the NPI after 1975 (72.09 km^2) indicates that melting trends have been accelerating, especially in the two largest outlet glaciers where the retreating rate has doubled in recent decades.

Between 1945 and 2005, the average retreating rate of 0.133 $km^2\ yr^{-1}\ gL^{-1}$ for the west side, from Grosse to Steffen glaciers, was four times larger than the average retreating rate of 0.033 $km^2\ yr^{-1}\ gL^{-1}$ for the east side, from Piscis to Exploradores glaciers. However, even if San Rafael and San Quintin glaciers are excluded from the west side, the retreating rate is still 0.082 $km^2\ yr^{-1}\ gL^{-1}$, more than twice that of the east side.

Although the general glacier variations trend of the NPI has been attributed to global warming, differences in the retreating rates between the east and the west sides may reflect the observed east–west ELA contrast (1979–2003). Because the disparate glacier variations in a given region can be explained by characteristics of individual glaciers such as size, steepness, and elevation, as well as mass turnover and geometry of the glacier drainage area (Furbish and Andrews, 1984), locational characteristics common to both ELAs and glacier variations would indicate glacier sensitivity to ELA oscillations and winter snow cover accumulation.

The larger retreating rates observed at the largest outlet glaciers (San Rafael, San Quintin, and Steffen) suggest topographic controls over the ELA since larger bare ice area variations are due to slight ΔZ_{ELA} over gentle accumulation areas. Therefore, glacier response to ΔZ_{ELA} would depend upon the location of the ELA, that is, in a gentle or steep accumulation area. Gentle accumulation areas are mostly found on the west and south sides. In addition, ΔZ_{ELA} becomes important even on the east side if the glacier is wide enough (Nef and Colonia glaciers) to make the ELA meander across the glacier surface. Different sensitivity to ELA shifts in neighboring glaciers with a gentle or steep accumulation area and the different contribution of calving activities have been discussed to explain contrasting variations of Upsala and Perito Moreno glaciers in the SPI (Aniya and Skvarca, 1992; Naruse et al., 1995).

Some outlet glaciers on the west side appear to have ELAs around 300 m lower than the previous estimates (1975), whereas a few of those located on the east side yielded the same range as in 1975. A similar result was obtained in 2002 by Rivera et al. (2007) using a single mid-summer ASTER image. Differences between the values derived for 1975 (Aniya, 1988) and the satellite-derived ELAs for the period from 1979 to 2003, in particular on the west side, may be attributed to different methods used and errors in both the topographic contours and the ASTER DEM.

On the east side of the NPI, on steep outlet glaciers nourished from the icefield, the location of the ELA above the ice falls was clearly recognized in the late-summer aerial survey. The León glacier has retreated very little, and because its ELA is located in a steep and crevassed area, even large ΔZ_{ELA} oscillations result in small bare ice area variations, thereby suggesting that it is rather

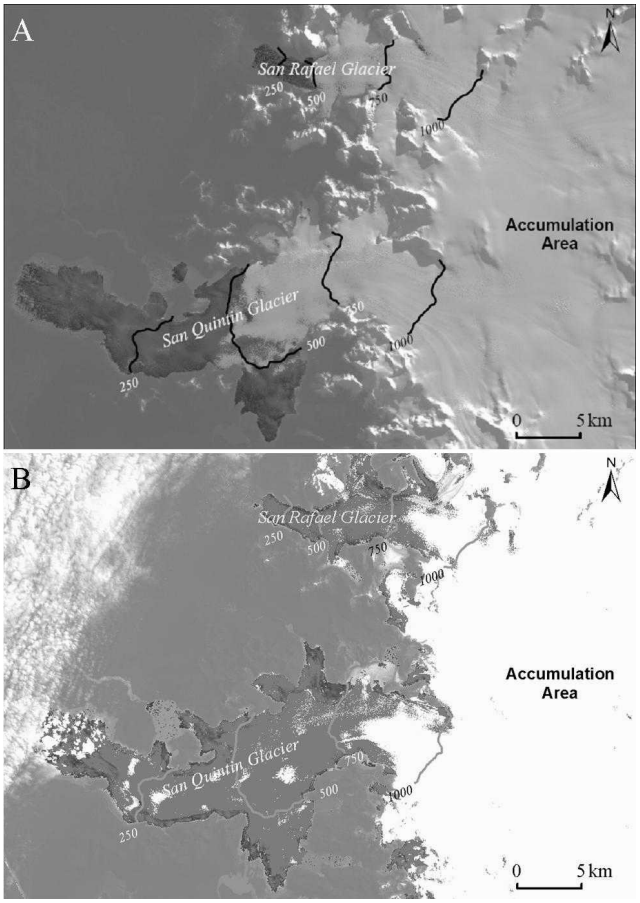

FIGURE 4. ***k*-means classification results for the neighboring San Rafael and San Quintin glaciers showing bare ice in winter ([A] 12 July 1999) and late-summer ([B] 08 March 2000). Bare ice (dark area) overlaid onto TM1. The lower part of the ablation area of both glaciers was found to be snow free in 1999, 2004, and 2005 (not shown); probably exposed to year-round ablation.**

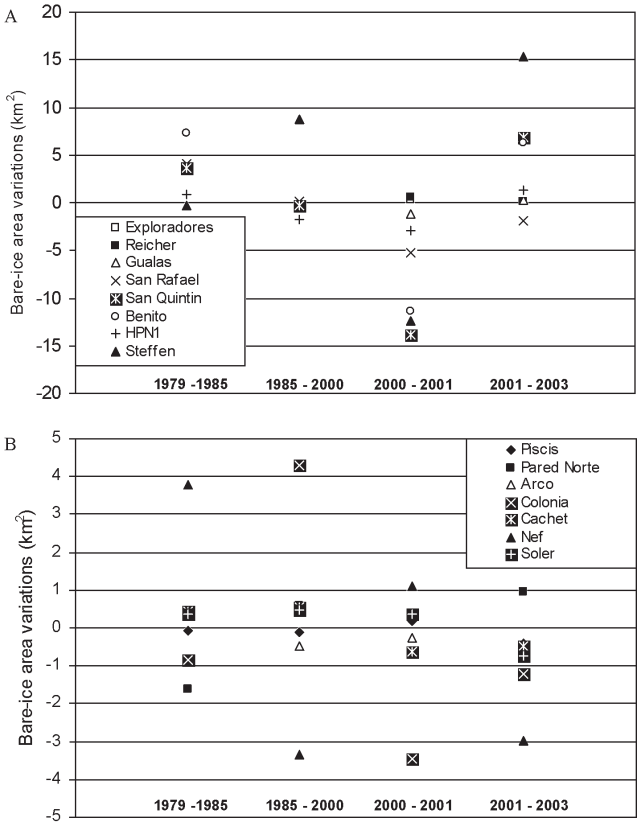

FIGURE 5. Interannual bare ice area variations for 15 major outlet glaciers from 1979 to 2003. (A) North, west, and south sides of the NPI; and (B) east side of NPI.

insensitive to ELA shifts. Among the glaciers on the east side, Fiero, Arco, and Piscis glaciers have retreated very little since 1945 (Aniya, 2007), and they can be considered stable because both ΔZ_{ELA} oscillations and bare ice area variations are negligible. However, even on the east side the topographic control over the ELA yields ΔZ_{ELA} oscillations of about 140 m for Nef and 106 m for Colonia glacier, suggesting that the size of outlets nourished from the plateau accounts for their higher sensitivity. Nef and Colonia retreated 5.03 km^2 and 2.09 km^2, respectively, in the 60-year interval (Aniya, 2007).

Meteorological data suggest that the 0°C isotherm over the plateau in late-summer is located at around 2000 m, which is about 700–1000 m higher than the observed ELAs. However, its lower elevation in winter (~900 m) is not sufficiently low to retain snow on the entire ablation area. Thus, on the west side, winter snow cover accumulation is not significant in the lower part of the ablation areas (see Fig. 6). Because at 47°S the snowline sensitivity (either ELA or TSL) depends primarily upon the mean annual temperature and secondarily upon precipitation (Kerr and Sugden, 1994), the higher sensitivity of glaciers in a wetter climate is due to a larger mass turnover (Oerlemans and Fortuin, 1992).

Rasmussen et al. (2007), using the National Center for Environmental Prediction/National Center for Atmospheric Research (NCEP/NCAR) reanalysis data, assumed a temperature (T) threshold of $T \leq +2$°C as the rain-snow divide in modeling the

TABLE 5

Transient snowlines (m) in winter 1999 and 2004 in Northern Patagonia Icefield.

Glacier name	Snout elevation*	1999	2004
Northern Side			
Grosse	*230*	700	501
Western Side			
Reicher	*80*	404	417
Gualas	*10*	450	313
San Rafael	*0*	446	440
San Quintin	*30*	510	257
Benito	*30*	424	116
HPN1	*50*	400	350
HPN2	*30*	354	466
HPN3	*170*	369	397
Southern Side			
Steffen	*25*	234	300
Eastern Side			
Piscis	*306*	covered	covered
Pared Sur	*200*	covered	covered
Pared Norte	*140*	425	covered
Arco	*246*	covered	covered
Colonia	*140*	423	covered
Cachet	*455*	covered	covered
Nef	*420*	560	covered
Soler	*350*	571	covered
León	*303*	530	covered
Fiero	*340*	563	covered
Exploradores	*250*	433	395

* From Aniya (1988).

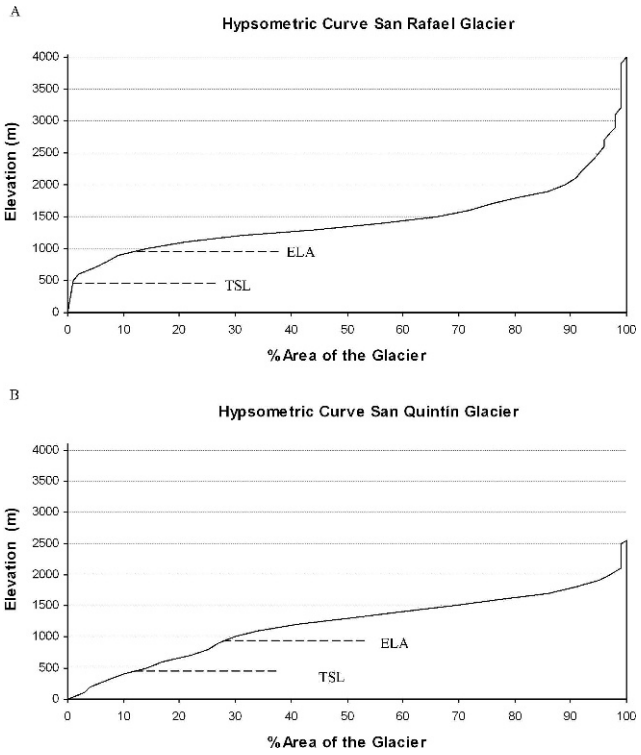

FIGURE 6. Hypsometric curve of San Rafael (A) and San Quintin (B) glaciers based upon ASTER DEM (2002) showing both the equilibrium line and the transient snowline (ice divides from Rivera et al., 2007).

snowfall in Patagonia at an elevation of 850-hPa (~1400 m). The sensitivity to temperature change indicates a decrease in snowfall of 9% with 1°C of warming and an increase in snowfall of 8% with 1°C of cooling. Since the precipitation is almost evenly distributed throughout year (Aniya et al., 2007), the vertical shift of the 0°C isotherm can cause both snow accumulation and melting at any time of year, a situation especially critical to mass balance on the west side where the accumulation areas are gentle.

For the two largest outlet glaciers of the NPI, we estimated the ELA at the central flow part to avoid the influence of local conditions (Rabatel et al., 2005). A maximum ΔZ_{ELA} of about 65 m for San Rafael and 70 m for San Quintin was observed from 1979 to 2003. Given the high sensitivity of the ELA to temperature changes at glaciers with high accumulation rates (Shiraiwa et al., 2002), this oscillation can be regarded as valid because it exceeds the vertical accuracy of the ASTER DEM, having caused substantial changes in the bare ice area. The continued ice thinning observed at both the glaciers (Aniya, 2001), in particular at San Quintin, may be in part attributed to the fact that, even in winter, bare ice in their ablation areas is largely free from overlying snow cover.

Conclusions

Despite the limited availability of optical imagery in Patagonia, the remote sensing technique proved to be useful for detecting changes in glacier surface conditions that can be correlated with glacier variations. Over the 24 years from 1979 to 2003, the ELA showed high year-to-year oscillations (ΔZ_{ELA}), causing larger bare ice area variations on the large and gentle glaciers. The topographic control over the ELA variation is suggested by the different variation patterns of glaciers whose ELAs are located in gentle or steep accumulation areas.

The larger retreating rates observed on the west side coincide with lower elevations of the ELAs (relative to the east side), larger interannual bare ice area variations, and ablation areas free from overlying winter snow cover. On the east side, glaciers that have retreated little coincide with a negligible ΔZ_{ELA} and minimal interannual changes.

Glacier variations reflect a higher sensitivity to ΔZ_{ELA} and winter snow cover accumulation on the west side as a combined result of the maritime influence, the lower elevation of glacier fronts, and gentle and large drainage areas. The likely year-round ablation in the lower part of westward outlet glaciers is an additional factor explaining the accelerated retreating rates, in particular at San Rafael and San Quintin glaciers.

Acknowledgments

This research was supported by grants provided by the Japanese Ministry of Education, Sport, Science and Culture (Project Number 15253001). Comments by Dr. Tomonori Tanikawa, Snow and Ice Research Laboratory, Kitami Institute of Technology (Japan), are appreciated. Pablo Iribarren (Dirección General de Aguas, Chile) prepared Figure 6. Detailed comments made by Professor Anne Jennings (INSTAAR) and two anonymous referees helped us improve the manuscript.

References Cited

Aniya, M., 1988: Glacier inventory for the Northern Patagonia Icefield, Chile, and variations 1944/45 to 1985/86. *Arctic and Alpine Research*, 20(2): 179–187.

Aniya, M., 1992: Glacier variation in the Northern Patagonia Icefield, Chile, between 1985/86 and 1990/91. *Bulletin of Glacier Research*, 10: 83–90.

Aniya, M., 1999: Recent glacier variations of the Hielos Patagónicos, South America, and their contribution to sea-level change. *Arctic, Antarctic, and Alpine Research*, 31(2): 165–173.

Aniya, M., 2001: Glacier variations of Hielo Patagónico Norte, Chilean Patagonia, since 1944/45, with special reference to variations between 1995/96 and 1999/2000. *Bulletin of Glaciological Research*, 18: 55–63.

Aniya, M., 2007: Glacier variations of Hielo Patagónico Norte, Chile, for 1944/45–2004/05. *Bulletin of Glaciological Research*, 24: 59–70.

Aniya, M., and Skvarca, P., 1992: Characteristics and variations of Upsala and Moreno glaciers, southern Patagonia. *Bulletin of Glaciological Research*, 10: 39–53.

Aniya, M., Naruse, R., Shizukuishi, M., Skvarca, P., and Casassa, G., 1992: Monitoring recent glacier variations in the Southern Patagonia Icefield, utilizing remote sensing data. *International Archives of Photogrammetry and Remote Sensing*, XXIX, part B7: 87–94.

Aniya, M., Sato, H., Naruse, R., Skvarca, P., and Casassa, G., 1996: The use of satellite and airborne imagery to inventory outlet glaciers of the Southern Patagonia Icefield, South America. *Photogrammetric Engineering and Remote Sensing*, 62(12): 1361–1369.

Aniya, M., Enomoto, H., Aoki, T., Matsumoto, T., Skvarca, P., Barcaza, G., Suzuki, R., Sawagaki, T., Sato, N., Isenko, E., Iwasaki, S., Sala, H., Fukuda, A., Satow, K., and Naruse, R., 2007: Glaciological and geomorphological studies at Glaciar Exploradores, Hielo Patagónico Norte, and Glaciar Perito Moreno, Hielo Patagónico Sur, South America, during 2003–2005 (GRPP03-05). *Bulletin of Glaciological Research*, 24: 95–107.

Boresjö Bronge, L., and Bronge, C., 1999: Ice and snow-type classification in the Vestfold Hills, East Antarctica, using Landsat-TM data and ground radiometer measurements. *International Journal of Remote Sensing*, 20(2): 225–240.

Casassa, G., Rivera, A., Aniya, M., and Naruse, R., 2002: Current knowledge of the Southern Patagonia Icefield. *In* Cassasa, G., Sepulveda, F., and Sinclair, R. (eds.), *The Patagonian Icefields: a Unique Natural Laboratory for Environmental and Climate Change Studies*. New York: Kluwer Academic/Plenum Publishers, 67–83.

Chavez, P. Jr., 1988: An improved dark-object subtraction technique for atmospheric scattering correction of multispectral data. *Remote Sensing of the Environment*, 24: 459–479.

Chinn, T. J., Heydenrych, C., and Salinger, M. J., 2005: Use of the ELA as a practical method of monitoring glacier response to climate in New Zealand's Southern Alps. *Journal of Glaciology*, 51(172): 85–95.

De Angelis, H., Rau, F., and Skvarca, P., 2007: Snow zonation on Hielo Patagónico Sur, Southern Patagonia, derived from Landsat 5 TM data. *Global and Planetary Change*, 59: 149–158.

Dozier, J., 1989: Spectral signature of Alpine snow cover from the Landsat Thematic Mapper. *Remote Sensing of the Environment*, 28: 9–22.

Fujiyoshi, Y., Kondo, H., Inoue, J., and Yamada, T., 1987: Characteristics of precipitation and vertical structure of air temperature in the northern Patagonia. *Bulletin of Glacier Research*, 4: 15–23.

Furbish, D. J., and Andrews, J. T., 1984: The use of hypsometry to indicate long-term stability and response of valley glaciers to changes in mass transfer. *Journal of Glaciology*, 30(105): 199–211.

Heo, J., and FitzHugh, T. W., 2000: A standardized radiometric normalization method for change detection using remotely sensed imagery. *Photogrammetric Engineering and Remote Sensing*, 66(2): 173–181.

Inoue, J., 1987: Wind regime of San Rafael glacier, Patagonia. *Bulletin of Glacier Research*, 4: 25–30.

Kerr, A., and Sugden, D., 1994: The sensitivity of the south Chilean snowline to climatic change. *Climatic Change*, 28: 255–272.

Khalsa, S. J. S., Dyurgerov, M., Khromova, T., Raup, B., and Barry, R., 2004: Space-based mapping of glacier changes using ASTER and GIS tools. *IEEE Transactions in Geosciences and Remote Sensing*, 42(10): 2177–2183.

Klein, A., and Isacks, B., 1999: Spectral mixture analysis of Landsat thematic mapper images applied to the detection of the transient snowline on tropical Andean glaciers. *Global and Planetary Change*, 22: 139–154.

Kuhn, M., 1989: The response of the equilibrium line altitude to climate fluctuations: theory and observations. *In* Oerlemans, J. (ed.): *Glacier Fluctuations and Climatic Change*. Dordrecht/Boston: Kluwer Academic Publishers, 407–417.

Matsuoka, K., and Naruse, R., 1999: Mass balance features derived from a firn core at Hielo Patagónico Norte, South America. *Arctic, Antarctic, and Alpine Research*, 31(4): 333–340.

Naruse, R., Aniya, M., Skvarca, P., and Casassa, G., 1995: Recent variations of calving glaciers in Patagonia, South America, revealed by ground surveys, satellite-data analyses and numerical experiments. *Annals of Glaciology*, 21: 297–303.

Oerlemans, J., and Fortuin, J. P. F., 1992: Sensitivity of glaciers and small ice caps to greenhouse warming. *Science*, 258(5079): 115–117.

Ohata, T., Kobayashi, S., Enomoto, H., Kondo, H., Saito, T., and Nakajima, C., 1985: The east–west contrast in meteorological conditions and its effect on glacier ablation. *In* Nakajima, C. (ed.), *Glaciological Studies in Patagonia Northern Icefield* Data Center for Glacier Research, Japanese Society of Snow and Ice, Report, 8: 52–56.

Ohmura, A., Kasser, P., and Funk, M., 1992: Climate at the equilibrium line of glaciers. *Journal of Glaciology*, 38(130): 397–411.

Paterson, W. S. B., 1994: *The Physics of Glaciers. Third Edition*. Oxford: Elsevier, 480 pp.

Rabatel, A., Dedieu, J. P., and Vincent, C., 2005: Using remote-sensing data to determine equilibrium-line altitude and mass-balance time series: validation on three French glaciers, 1994–2002. *Journal of Glaciology*, 51(175): 539–546.

Rasmussen, L. A., Conway, H., and Raymond, C. F., 2007: Influence of upper air conditions on the Patagonia icefields. *Global and Planetary Change*, 59: 203–216.

Rees, W. G., 2006: *Remote Sensing of Snow and Ice*. Boca Raton: Taylor & Francis, 285 pp.

Rignot, E., Rivera, A., and Casassa, G., 2003: Contribution of the Patagonia icefields of South America to sea level rise. *Science*, 302(5644): 434–437.

Rivera, A., Casassa, G., Bamber, J., and Kääb, A., 2005: Ice-elevation of Glaciar Chico, southern Patagonia, using ASTER DEMs, aerial photographs and GPS data. *Journal of Glaciology*, 51(172): 105–112.

Rivera, A., Benham, T., Casassa, G., Bamber, J., and Dowdeswell, J., 2007: Ice elevation and areal changes of glaciers from the Northern Patagonia Icefield, Chile. *Global and Planetary Change*, 59: 126–137.

Shiraiwa, T., Kohshima, S., Uemura, R., Yoshida, N., Matoba, S., Uetake, J., and Godoi, M. A., 2002: High net accumulation rates at Campo de Hielo Patagónico Sur, South America, revealed by analysis of a 45.97 m long ice core. *Annals of Glaciology*, 35: 84–90.

Wada, Y., and Aniya, M., 1995: Glacier variations in the Northern Patagonia Icefield between 1990/91 and 1993/94. *Bulletin of Glacier Research*, 13: 111–119.

Warren, C., and Aniya, M., 1999: The calving glaciers of southern South America. *Global and Planetary Change*, 22: 59–77.

Warren, C., and Sugden, D., 1993: The Patagonian icefields: a glaciological review. *Arctic and Alpine Research*, 25(4): 316–331.

Warren, C., Glasser, N., Harrison, S., Winchester, V., Kerr, A., and Rivera, A., 1995: Characteristics of tidewater calving activity at Glaciar San Rafael, Chile. *Journal of Glaciology*, 41(138): 273–289.

Williams, R. S., Hall, D. K., and Benson, C. S., 1991: Analysis of glacier facies using satellite techniques. *Journal of Glaciology*, 37(125): 120–128.

Yamada, T., 1987: Glaciological characteristics revealed by 37.6-m deep core drilled at the accumulation area of San Rafael Glacier, the Northern Patagonia Icefield. *Bulletin of Glacier Research*, 4: 59–67.

MS accepted January 2009